Absorption studies of excimer transitions in Cs–noble-gas and Rb–noble-gas molecules*

G. Moe, A. C. Tam, and W. Happer
Columbia Radiation Laboratory, Department of Physics, Columbia University, New York, New York 10027
(Received 15 March 1976)

The new excimer emission bands from laser-excited and discharge-excited alkali–noble-gas systems we recently reported are observed in absorption for Cs and Rb, with noble-gas densities between 1 and 10 amagats. The absorption bands observed correspond to transitions from the unbound Σ molecular ground state to bound or free Σ and Π excited states which are correlated with low-lying S and D excited alkali atoms, so that the corresponding atomic transitions are forbidden. Quantitative reduced absorption coefficients (k_ν divided by the vapor densities) are derived from the observed spectra and have peak values of the order of 4×10^{-38} cm^5 for the heaviest noble gas, xenon. A comparison is made with the spectra that would be expected from the adiabatic potential curves recently calculated by Pascale and Vandeplanque, with the conclusion that they have exaggerated the repulsion in certain excited Σ states.

INTRODUCTION

The broadening and shift of the resonance lines of alkali-metal atoms by noble gases have been known and studied for many years. There has been a resurgence of interest in the spectroscopy of these lines in recent years, however, since Hedges, Drummond, and Gallagher[1] demonstrated that light radiated in the far spectral wings of these lines, as much as 1000 Å from line center, can be used to determine the molecular potential curves for alkali–noble-gas pairs. The results of the recent studies indicate that although the alkali atom and noble-gas atom do simply repel each other (except for a very weak Van der Waals attraction) when the alkali atom is in its ground $^2S_{1/2}$ state, the two atoms may bind together to form a molecule when the alkali atom is in an excited P state.

Recently we reported the observation of new emission[2] and absorption[3] bands which indicate that this can also happen when the alkali atom is in an excited S or D state. In that case a forbidden atomic transition becomes an allowed molecular transition, and instead of a spectral wing or satellite on an allowed transition peak, one observes isolated bands shifted considerably from the wavelength corresponding to the forbidden transition. These transitions may be of interest for excimer laser purposes.[4] The bands are also of interest because they provide information on the interatomic potentials, which, in turn, are related to such collisional processes as depolarization, quenching, and excitation transfer, which have been most widely investigated for alkali–noble-gas atom pairs.

We have since measured the absorption coefficient of Cs and Rb with all the noble gases in the visible and near-infrared regions of the spectrum. Here we report the results of that investigation, together with a largely qualitative discussion of what the spectra imply about the nature of the excited-state potential curves. The spectra appear to be at considerable variance with those that would be expected from presently available theoretical potentials.

EXPERIMENT

The present absorption studies were made using a standard commercial dual beam spectrophotometer (Cary Model 14, Applied Physics Corp.), modified slightly to accept an oven containing absorption cells of alkali-resistant aluminosilicate glass (Corning 1720). The full width at half-maximum of the instrument function is approximately 10 Å. The absorption cells were cylindrical, 2.1 cm i.d. by 5 cm long. Before filling the cells we baked them at 500 °C for at least 8 h under a vacuum of 10^{-6} Torr. Then a substantial amount of alkali metal was distilled in from a break-seal ampule, noble gas was admitted, and the cells were sealed off. Noble-gas densities in excess of 1 amagat were obtained by placing one end of the cell in liquid nitrogen during sealoff.

Figure 1 shows absorption spectra of Cs in vacuum and Cs with ~3 amagat of each of the noble gases at 371 °C. The pure Cs absorption spectrum (bottom trace) is primarily due to Cs_2 dimer bands, although the second and third atomic principal resonance lines are clearly visible, and is consistent with the data of Lapp and Harris[5] and Wechsler.[6] Absorption by the aluminosilicate glass cell wall at short wavelengths was found to increase at high temperatures and is responsible for a gradual rise at the extreme left-hand side of the figure.

To separate the absorption due to the alkali–

noble-gas molecules from that of the dimers we digitized separate absorption traces obtained at the same temperature for cells with no noble gas (bottom trace) and with noble gas, then computed the absorption coefficient for each and substracted the dimer absorption coefficient from that of the mixture. This was done for a large number of absorption spectra of many cells with varying noble-gas densities (ranging from 0.9 to 11.6 amagat for Xe, for example) and temperatures from 325 to 405 °C. A minicomputer was employed to facilitate the reduction of this large amount of data. The reduced absorption coefficient (absorption coefficient divided by the atomic alkali and noble-gas densities) was plotted by the minicomputer, then a smooth curve was drawn by hand through the discrete points. This process, as well as our subsequent averaging of different traces, resulted in the smoothing of the noise fluctuations in the original strip chart recordings, which would normally serve to indicate the extent of uncertainty. We have therefore indicated in the figure captions the estimated uncertainties. We have computed the Cs vapor density from the measured cell temperature using the formulas of Ditchburn and Gilmour[7]; this and uncertainty in the temperature measurement introduce an additional systematic uncertainty of ~±25% in the magnitude (vertical scale factor) of the reduced absorption coefficients.

Figure 2 shows the reduced absorption coefficient for the yellow bands of Cs in Ne, Ar, Kr, and Xe. These curves are very similar to the emission spectra reported previously.[2] The bands are due to transitions between Cs–noble-gas molecular states correlated with the 7*S* excited state and 6*S* ground state in atomic Cs. The data shown in Fig. 2 were obtained at 371 °C. We carefully studied the temperature dependence of the CsXe reduced absorption coefficient from 325 to 405 °C and found no observable change with temperature. Thus the absorption coefficient is directly proportional to the Cs density. For the other noble gases we simply ascertained that there is no observable change in the wavelength of the peak or the qualitative shape of the band with temperature.

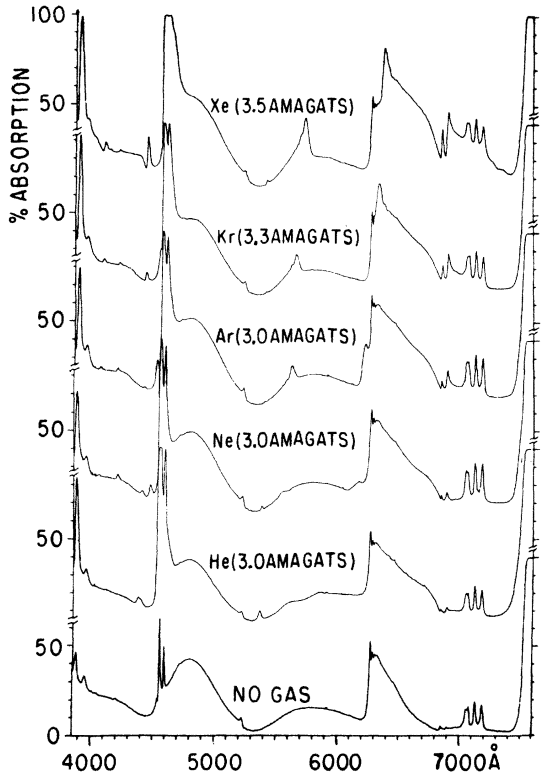

FIG. 1. Absorption spectra of Cs–noble-gas systems and Cs in vacuum. The absorption path length is 2.0 cm and the temperature is 371 °C. The ordinate is linear, with each successive trace displaced upward by 60(%).

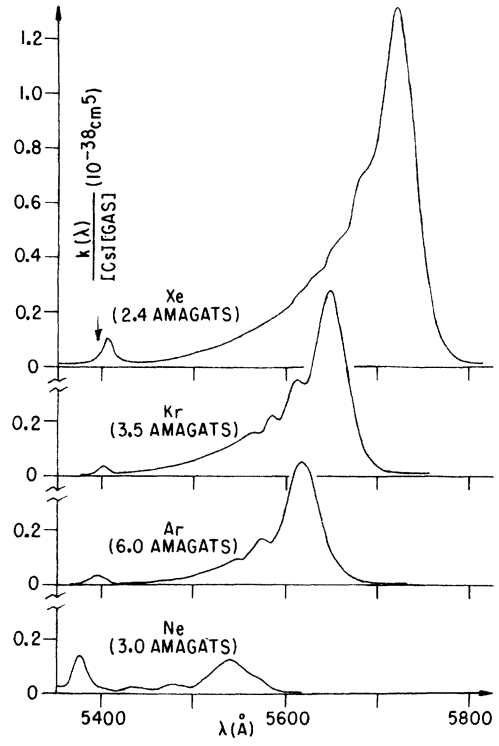

FIG. 2. Reduced absorption coefficients for the Cs–noble-gas yellow band. The arrow indicates the position of the forbidden atomic Cs 6*S*–7*S* transition at 5394 Å. The uncertainty is $\pm 0.03 \times 10^{-38}$ cm^5, with an additional ±25% systematic uncertainty in the Cs density, which, as discussed in the text, affects the magnitude but not the shape of the bands. The resolution (width of the instrument function) is approximately 10 Å.

The Ne trace has a particularly large uncertainty, because the effect is small and we were unable to freeze the Ne to produce densities greater than 3 amagat. We have included it for completeness, but it is observed much more clearly in the emission data reported previously.[2] As we have previously noted,[3] these absorption spectra are slightly more heavily weighted toward the blue than the corresponding emission spectra, as one would expect because of the Boltzmann population factors in the ground and excited states. The positions of the peaks coincide, within experimental uncertainty, with those previously observed in emission.

Figure 3 shows the effect of increasing noble-gas density on the CsXe yellow band. These spectra are normalized to the same peak height, since they were taken with different cells, and the differences of $\lesssim 10\%$ in height mainly reflected uncertanity in noble-gas density. As we have previously noted,[3] the peak broadens and shifts toward the red at the rate of 2.1(4) Å/amagat as a result of having more than a single noble-gas atom near the Cs atom. Within the uncertainty of the noble-gas density and apart from this broadening and shifting at high noble-gas densities, the absorption coefficient $k(\lambda)$ is proportional to the noble-gas density.

The absorption spectra shown in Fig. 1 also display substantial noble-gas–induced absorption bands in the region 6000–7400 Å, as has been noted previously.[3,8] These bands, which partially overlap Cs_2 dimer absorption bands, are correlated with the $5D$ level in atomic Cs. Figure 4 shows the Cary absorption traces for this region in more detail for the case of CsAr. The reduced absorption coefficient, with the Cs_2 absorption coefficient subtracted as previously described, is shown in Fig. 5. The traces shown represent an average of data obtained at two temperatures, 325 and 371 °C, for the given pressures. They were smoothed and checked using additional data obtained with noble-gas pressures ranging from 0.9 to 11.6 atm. The higher pressures had the best signal-to-noise ratio and differed only in a slight broadening and decrease in height of the highest peak.

The undulations near this peak are very small in the original data, barely above the noise, as can be seen in Fig. 4. They are present in all the traces, but, particularly in the case of Ar, they are small and occur in a region where there is considerable structure in the underlying Cs_2 bands. Our method of analyzing and presenting the data has made these undulations appear somewhat more distinct than our confidence warrants, and we do not wish to claim more than that these undulations are probably present in the noble-gas–induced absorption spectra and qualitatively correct as shown. The primary reason for our uncertainty is that the data were not obtained over a sufficiently wide range of temperatures to demonstrate with certainty that small noble-gas–induced features such as these undulations are not noble-gas–in-

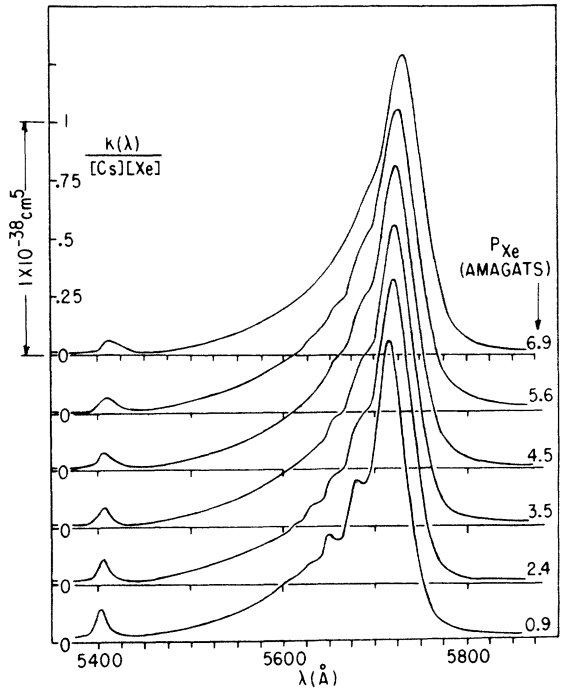

FIG. 3. The change in the shape of the CsXe yellow band with increasing noble-gas density. The curves are normalized to the height of the 2.4-amagat trace.

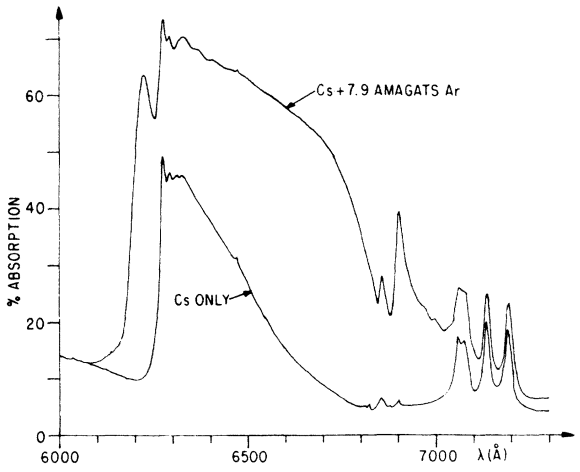

FIG. 4. Absorption spectra of Cs in vacuum and Cs with 7.9-amagat Ar at 371 °C, path length of 2.0 cm, and Cs density of 1.40×10^{17} cm^{-3}.

duced changes in the underlying Cs_2 dimer bands. The range of temperatures and the quality of the data are sufficient, however, to demonstrate that the gross features of the bands are not due to noble-gas–induced changes in the Cs_2 bands. For example, the height of the most blue-shifted peak is the same within an uncertainty of 4% for data obtained at 325 and 371 °C for CsXe and CsKr. The alkali density increases by a factor of 2.5 over this temperature range,[7] but the Cs_2 density increases even more rapidly; the ratio of densities $[Cs_2]/[Cs]$ increases by a factor of about 1.5.[9] Thus the fact that the absorption coefficient at the peak is proportional to the Cs density within an experimental uncertainty of 4% for the cases of Xe and Kr, for example, demonstrates that these red bands are associated with Cs, not Cs_2. A similar statement applies to the yellow CsXe band. The lack of temperature dependence also provides an upper bound on the magnitude of the lower potential at the internuclear separation at which the transition takes place, as will be discussed later.

The absorption spectra shown in Fig. 1 also exhibit noble-gas–induced features in the region 3900–4555 Å, between the second and third principal resonance lines of Cs. Figure 6 shows the raw data for this region in more detail for the case of CsXe (top trace) and the reduced absorption coefficient obtained by our subtraction procedure for the noble gases Ne through Xe. As for the red and yellow bands, we have indicated an uncertainty in the figure caption that does not include an additional systematic uncertainty of about 25% in the magnitude or scale factor of the absorption coefficient due to uncertainty in the vapor densities. The uncertainty is large enough so that, particularly for the lighter noble gases, only the gross features are significant. These features are again peaks which shift systematically towards the red with increasing noble-gas molecular weight (and polarizability). These peaks presumably result from transitions between molecular terms correlated with the Cs ground state and $6D$, $8S$, and $4F$ excited states, as well as $7P$ and $8P$. Small features in the spectrum of CsXe near the Cs $6S$-$6D$ doublet have been reported by Lapp[10] in absorption and by Gwinn *et al.*[11] in emission.

We have also measured the absorption coefficient of Rb in the noble gases. The raw absorption spectra are shown in Fig. 7, with the noble-gas densities indicated. The temperature was 370 °C,

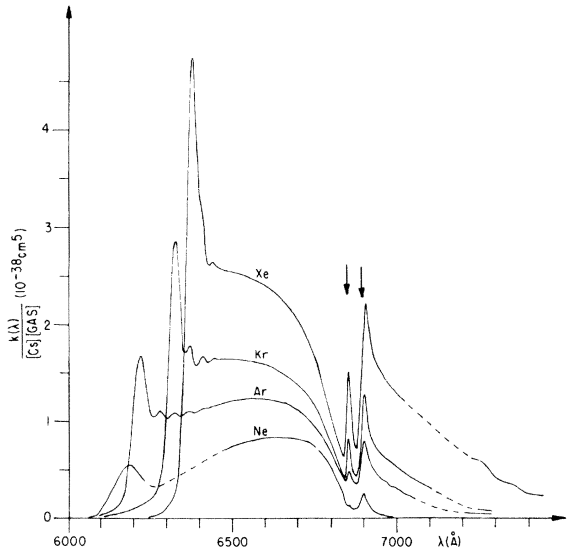

FIG. 5. Reduced absorption coefficients for the Cs–noble-gas red bands. The noble-gas densities are 4.5, 5.0, 7.9, and 3.0 amagat for Xe, Kr, Ar, and Ne, respectively. The arrows indicate the wavelengths of the forbidden Cs atomic $6S_{1/2}$-$5D_{5/2,3/2}$ transitions at 6849 and 6895 Å. The uncertainty is $\pm 0.1\times 10^{-38}$ cm^5, subject to an additional ±25% uncertainty in the Cs density which does not affect the shape. The dashed lines indicate regions where the data are much more uncertain because of the overlapping Cs_2 bands.

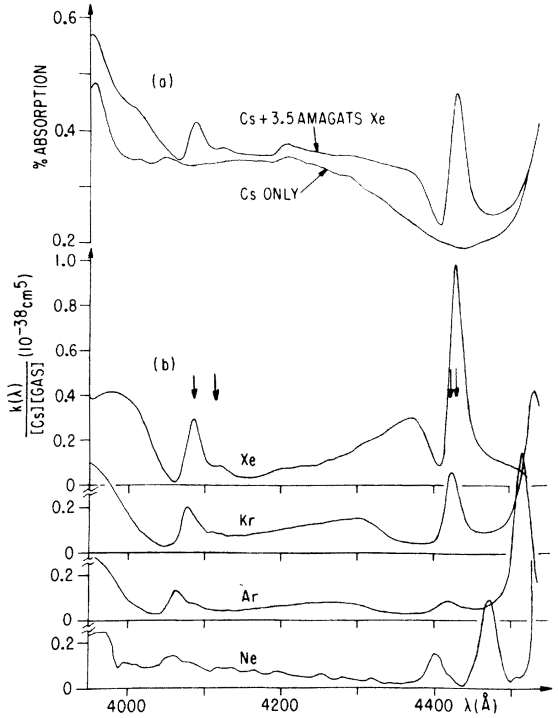

FIG. 6. Cs–noble-gas absorption bands in the blue. The noble-gas densities for the traces shown are 3.0, 7.9, 5.5, and 4.0 amagat for Ne, Ar, Kr, and Xe, respectively. The arrows indicate the wavelengths of the forbidden atomic Cs $6S$-$4F$, $6S$-$8S$, and $6S$-$6D_{5/2,3/2}$ transitions, from left to right. The uncertainty (see discussion in text) is $\pm 0.05\times 10^{-38}$ cm^5.

which corresponds to a Rb vapor density of 9.94×10^{16} cm^{-3}.[7] The bottom trace shows the absorption due to rubidium alone, which is largely due to Rb_2 molecules, although the second principal resonance lines of Rb are also visible. The results of subtracting the Rb_2 absorption coefficient from that of the Rb–noble-gas systems is shown in Fig. 8. The absorption bands are correlated with the forbidden 4966-Å $5S$-$6S$ and 5165-Å $5S$-$4D$ forbidden transitions in atomic Rb and correspond to the green bands we have previously reported[2] in emission. They have been reported qualitatively in absorption by Besombes *et al.*[12] at a much higher temperature (950 °C) and discussed by Granier *et al.*[13] They associate these bands solely with the quadrupole $5S$-$4D$ transition. Our Cs data indicate that absorption bands associated with the forbidden S-S transitions in the alkali atoms can be comparable in strength with those associated with S-D transitions.

DISCUSSION

Several of the most prominent absorption bands in the spectra have similar characteristics; a broad continuous absorption band, which starts with small absorption at the wavelength which corresponds to a forbidden transition in the alkali atom, increases gradually with separation from this forbidden transition wavelength, reaches a definite peak, and then falls off sharply on the far side of the peak. The Cs–noble-gas yellow bands in Fig. 2, which are red shifted from the 5394-Å forbidden $6s$-$7s$ transition in atomic Cs, have these characteristics, as do the prominent bands in Fig. 5 which extend toward the blue from the wavelength of the $6^2S_{1/2}$-$5^2D_{5/2}$ transition at 6849 Å. The wavelengths of the peaks which terminate these bands do not shift appreciably with temperature, as one would expect them to shift if they were simply determined by Boltzmann population factors, and they occur at the same wavelength in emission as in absorption. Most of these characteristics are similar to those of the satellites and spectral wings observed on allowed transitions. These satellites are understood in terms of the adiabatic potential curves to result from extrema in the difference between the upper and lower potentials. Similarly, it is

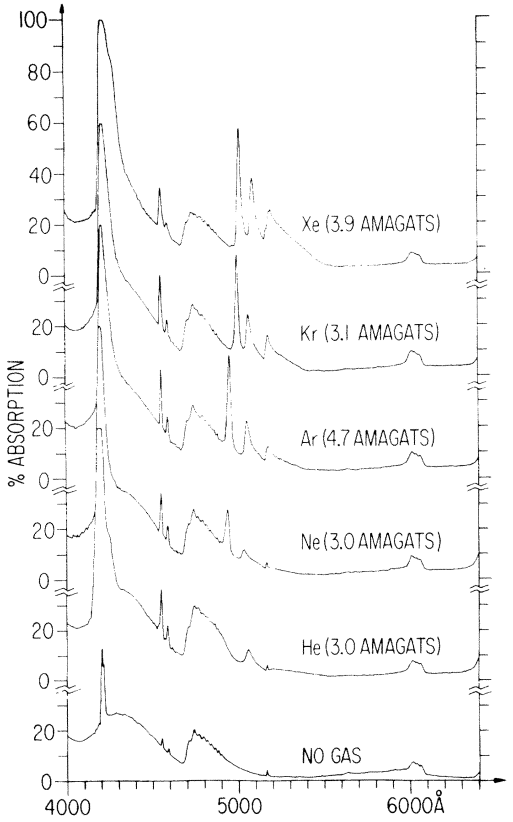

FIG. 7. Absorption spectra of the Rb–noble-gas systems and Rb in vacuum at 370 °C. The path length is 2.0 cm.

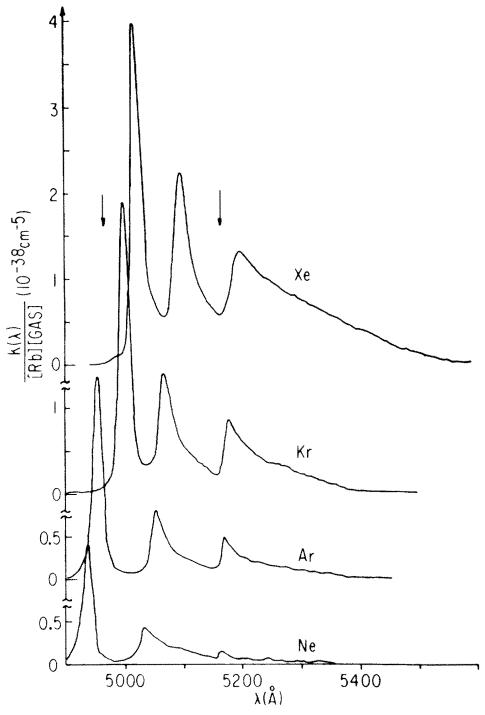

FIG. 8. Reduced absorption coefficients for the Rb–noble-gas green bands. The uncertainty is ±0.1 $\times 10^{-38}$ cm^5, with an additional ±35% systematic uncertainty in the Rb density which does not affect the shape. The arrows indicate the wavelengths of the forbidden atomic Rb $5S$-$6S$ and $5S$-$4D$ transitions at 4966 and 5165 Å, respectively.

very reasonable to associate the Cs–noble-gas peaks discussed above, as well as the two shortest-wavelength Rb–noble-gas peaks in Fig. 8, with extrema in the difference potentials. The wavelengths of these peaks are tabulated in Table I.

Gallagher and co-workers have demonstrated that for the case of allowed transitions an extension of the quasistatic theory originally formulated by Holtzmark and developed by many others can be used very successfully to determine adiabatic potentials from the continuum spectra.[1,14,15] In this simple semiclassical theory the density of noble-gas atoms at a distance R from the alkali atom in equilibrium is given by a simple Boltzmann distribution

$$n(R) = n_0 e^{-V_l(R)/kT}, \tag{1}$$

where V_l refers to the lower (ground-state) potential (assumed to be zero at $R = \infty$), V_u refers to the excited-state potential, and n_0 is the background noble-gas density (the notation is that of Ref. 1). The absorption coefficient for the transition at the temperature T is then given by

$$k_\nu(T) = C n_0 N_l R^2 A(R) e^{-V_l(R)/kT} \Big/ \nu^2 \left| \frac{d\nu}{dR} \right| \tag{2}$$

in the approximation that the density n_0 is low enough that only binary collisions need be considered. N_l is the density of alkali atoms in the ground state and C is an unimportant constant. $A(R)$ is the transition moment, which for allowed transitions is assumed independent of the internuclear separation R and proportional to ν^3. For forbidden atomic transitions the dependence of A on R must be known, where R and the frequency ν are related by the equation $h\nu = V_u(R) - V_l(R)$.

According to Eq. (2) an extremum in the difference potential, $d\nu/dR = 0$, causes the absorption coefficient to go to infinity. This singularity is an artifact of the quasistatic theory. It is a result of the use of the classical Franck-Condon principle, which says that electronic transitions take place vertically from one potential curve to another. This requirement that nuclear momentum be conserved in a transition is only approximate. The quasistatic theory thus gives poor results with very light nuclei (in particular, for He)[14] and in the immediate neighborhood of the satellite which is associated with an extremum in the difference potential.

The singularity associated with the extremum is removed in the more sophisticated theories recently developed by Szudy and Baylis[16] and Sando and Wormhoudt[17] and discussed by Carrington and Gallagher.[18] Their results are not directly applicable to the present case, because the transition moment is assumed to be constant, although it should be possible to include the dependence of A on R, at least in the low-density limit.[16] In addition, the WKB approximation used in these calculations may give poor results in the present case if the extremum occurs at small R, where the ground-state potential is repulsive and the orbits have classical turning points.[18] Nevertheless, the calculations do suffice to provide a qualitative picture of the shape of the peak in the spectrum which is associated with an extremum in the difference potential, and that will suffice for the present discussion. They show that the peak is finite and rounded and may be shifted by as much as a few tens of angstroms from the position of the quasistatic infinity, and that some absorption or emission occurs in the classically forbidden region beyond the quasistatic infinity, although it still falls off very sharply on the far side. Under some conditions interference effects may give rise to undulations on the side of the satellite nearest the isolated-atom transition wavelength. For attractive excited states, of course, vibrational structure may also cause undulations.

We do not know the dependence of the transition moment on R. For this and other reasons discussed above, we cannot simply compute from a given set of potential curves the resulting absorption spectrum, and of course we cannot invert the spectra to obtain the potentials. We shall see, however, that a good deal of useful information concerning the potential curves can be obtained without doing such a detailed calculation, simply from such gross features as the positions of the major bands and peaks and some knowledge of their dependence on temperature (the ground-state potential curves are known).[1,14] For this purpose (and excepting He) the simple quasistatic theory,

TABLE I. Wavelengths (in Å, measured in air, with uncertainties in parentheses) of the peaks of absorption bands observed in Cs–noble-gas and Rb–noble-gas molecules. The noble-gas density is 3.0 amagat. The (forbidden) alkali-atom transition nearest the band is given in the first column. The red shift with pressure is indicated in square brackets (in Å/amagat) for those peaks in which it was large enough to be measurable, with an uncertainty of ±0.4 Å/amagat.

		Ne	Ar	Kr	Xe
Cs	6S-7S	5543(8)	5618(3)	5646(3) [1.5]	5721(3) [2.1]
	6S-5D	6178(10)	6219(3)	6327(3) [0.9]	6376(3) [1.2]
Rb	5S-6S	4942(6)	4956(3)	5002(3)	5018(2)
	5S-4D	5033(6)	5055(3)	5071(3)	5093(2)

with the frequency given in terms of the difference potential by $h\nu = V_u(R) - V_l(R)$ and the temperature dependence given by a Boltzmann distribution, together with the above qualitative picture of the peaks associated with extrema in the difference potential, is sufficient.

The association of the peaks with extrema in the difference potentials becomes both very reasonable and interesting when viewed in the light of the adiabatic potential curves recently calculated by Pascale and Vandeplanque.[19] This is, as far as we know, the only calculation of molecular terms in the heavy-alkali–noble-gas molecules above those correlated with the first alkali P state. It is a semiempirical potential-model calculation extending the work of Baylis,[20] who considered only the lower states. The adiabatic potential curves are obtained by finding the eigenvalues of an effective Hamiltonian, which depends on R, for the valence electron alone. The effects of the Pauli exclusion principle are simulated by two pseudopotential terms. One of these provides for "core-core" repulsion, and the other tends to exclude the valence electron from the neighborhood of the noble-gas atom. We note that molecular states which have the electron primarily in a σ orbital, which we call Σ states, are uniquely sensitive to this valence-electron pseudopotential. The s orbital has spherical symmetry and the $p\sigma$, $d\sigma$, etc. orbitals have a lobe of the electronic wave function extending along $\vec{R}$ toward the noble-gas atom, so that they are sensitive to the repulsion at relatively large R.[20] The other states, in which the electron is mainly in a π or δ orbital, for example, have a node in the direction of $\vec{R}$ and the alkali atom can get much closer to the noble-gas atom before the repulsion is strongly felt. [The coupling in the alkali–noble-gas molecules progresses from Hund's case c at large R towards Hund's case a, in which the orbital and spin angular momenta of the electron are decoupled at small R. We use a notation ($7s\Sigma$, $5d\Sigma$, etc.)[20] appropriate to Hund's case a because it simplifies the discussion, even though the coupling may not be pure because of the large spin-orbit interaction in the heavy alkalies.]

The most striking features of the potential curves calculated by Pascale and Vandeplanque (PV) are the pronounced perturbations and avoided crossings in the excited Σ potentials, in which the part played by the repulsive interaction discussed above is apparent. To illustrate this we have reproduced in Figs. 9 and 10 some of the PV potentials for RbXe and CsXe, respectively. A very pronounced perturbation and avoided crossing of the RbXe $6s\Sigma$ term with terms correlated with the Rb $6P$ state is apparent in Fig. 9. Figure 10

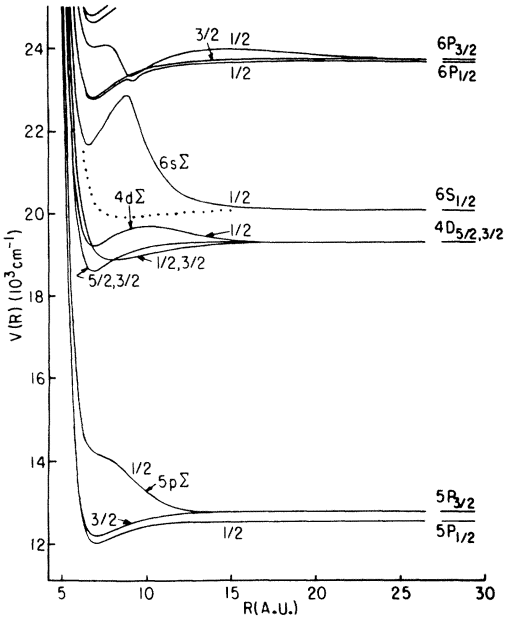

FIG. 9. Theoretical adiabatic potential curves for RbXe reproduced from Pascale and Vandeplanque, Ref. 19 (solid lines). The dotted line indicates a $6s\Sigma$ potential curve compatible with our interpretation of the absorption spectra.

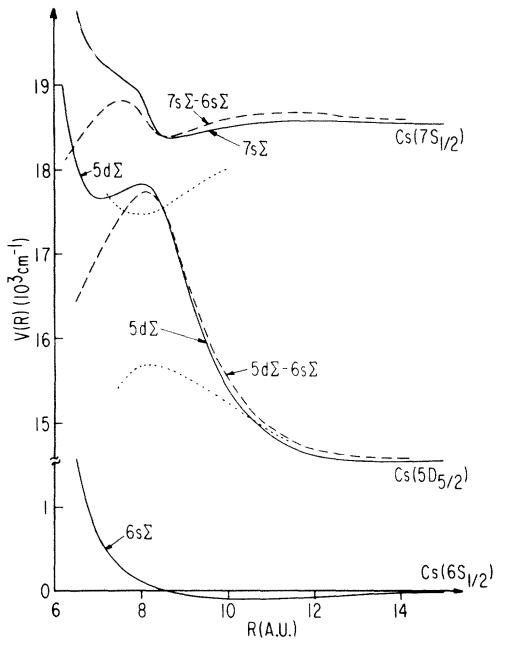

FIG. 10. Theoretical adiabatic potential curves (solid lines) for CsXe from Ref. 19, with the corresponding difference potentials (dashed lines). The dotted lines show difference potentials compatible with our spectra, as discussed in the text.

shows the avoided crossing between the $5d\Sigma$ term of CsXe and the $7s\Sigma$ term just above it (solid lines). This results in a bump or shoulder on the $5d\Sigma$ potential and relatively shallow and distorted well in the $7s\Sigma$ potential. The difference potentials for the transitions from these two potential curves to the ground state are also shown in Fig. 10 (dashed lines), as is the ground-state potential itself.

We have focused this discussion on the highly perturbed Σ potential curves, because the most prominent bands in our absorption spectra are associated with these terms, and because the dramatic perturbations would have such gross and predictable effects on the absorption spectra that a qualitative comparison is easy to make and yet very productive. Consider first the $5d\Sigma$-$6s\Sigma$ transition in CsXe. The difference potential (lower dashed line in Fig. 10) is equal to the energy of the photon that would be emitted at each value of R, and if we follow this curve in from large R we see that the frequency shifts toward the blue until the difference potential reaches a maximum at about 8.2 a.u. and turns down. This would result in a continuous absorption band starting from the wavelength of the isolated Cs-atom $6S_{1/2}$-$5D_{5/2}$ quadrupole transition (6849 Å) and extending toward the blue, increasing in intensity (as the transition moment increases) until it terminates in a peak at approximately the wavelength corresponding to the difference potential, 5634 Å. This is just what we see in the experimental spectrum in Fig. 5, except that the sharp peak associated with the extremum, which occurs at 6376 ± 3 Å, is shifted much less toward the blue (1082 cm^{-1}) than is expected from the PV potentials (3153 cm^{-1}). Thus the experimental spectra indicate that the extremum in the $5d\Sigma$-$6s\Sigma$ difference potential occurs at approximately 15.68×10^3 cm^{-1}. We have sketched an example of such a difference potential in Fig. 10 (lower dotted line). Of course it is not unique—so far we have determined only that the height of the extremum is $\sim 15.68 \times 10^3$ cm^{-1}. We can, however, use the temperature dependence (or rather lack of temperature dependence) of the magnitude of the experimental absorption coefficient together with the known ground-state potential curve to get information about the value of R at which the extremum occurs, and thereby partially separate the contributions from the upper and lower potentials to the difference potential. The PV ground-state potentials are, for our purposes, in satisfactory agreement with experiment.[1,14]

To a first approximation the magnitude of the reduced absorption coefficient should depend exponentially on the temperature according to the Boltzmann population factor $e^{-V_l(R)/kT}$ in Eq. (2).[18] Our study of the temperature dependence is restricted to Xe and Kr, where the uncertainty is the smallest. The change in magnitude of the peak in the $5d\Sigma$-$6s\Sigma$ band between 325 and 370 °C was less than the experimental uncertainty of 6% (this uncertainty applies to measurements made with the same cell at different temperatures, and we have added 2% for uncertainty in the slope of the vapor density versus temperature curve). This implies that the extremum in the $5d\Sigma$-$6s\Sigma$ difference potential occurs at an R such that $V_l(R) \lesssim 350$ cm^{-1} for CsXe and CsKr, and the extremum cannot occur at an R much smaller than that shown by the dotted line in Fig. 10.

As we have indicated with the dotted line, the $5d\Sigma$ potential curve must be far less repulsive than the theoretical PV potential. This implies that it stays relatively far away from the $7s\Sigma$ term, so that the mutual perturbation and avoided crossing of these two terms is greatly reduced, and the $7s\Sigma$ term must have a well considerably deeper than that exhibited in Fig. 10. The absorption and emission spectra clearly demonstrate that this is the case.

The peak of the yellow CsXe band in Fig. 2 at 5721 Å (for Xe density 3.0 amagat) is shifted by 1061 cm^{-1} from the forbidden 7S-6S atomic Cs transition, which would occur at 5394 Å. This 1061 cm^{-1} is the sum of the repulsion in the ground-state potential curve and the depth of the well in the $7s\Sigma$ potential at the R corresponding to the wavelength of the peak. To put an upper bound on the magnitude of the ground-state potential $V_l(R)$, we again look to the temperature dependence of the absorption coefficient. The magnitude of the reduced absorption coefficient at the peak of the yellow band for CsXe was unchanged over the temperature range 325–405 °C, with an uncertainty of 3% (comparing data for the same cell at different temperatures to eliminate uncertainty in the noble-gas density). Following our previous reasoning, and taking into account the uncertainty in the change in Cs vapor density, this implies that $V_l(R) \lesssim 173$ cm^{-1}. Thus the CsXe $7s\Sigma$ potential well must be at least ~ 890 cm^{-1} deep.

As was previously mentioned, these Cs–noble-gas yellow bands also appear to be associated with extrema in the difference potentials, at least for the heavier noble gases. For CsXe this means the extremum lies approximately 1061 cm^{-1} below the frequency of the forbidden 7S-6S atomic transition. The PV potentials would give a red shift of only 136 cm^{-1}. In addition they give two additional extrema with blue shifts which would cause additional peaks not found in the experimental data. The upper dotted line in Fig. 10 shows a differ-

ence potential which would be compatible with this simple analysis of the absorption spectra. Again, it is not unique, and the precise shape cannot be determined without knowing the variation of the transition moment with R.

The preceding discussion demonstrates that for the case of CsXe there are substantial differences between the absorption spectra we observe and those that would be expected from the PV potentials for the terms correlated with $7\,^2S_{1/2}$ and $5\,^2D_{5/2}$ in Cs, that a qualitative discussion is sufficient to illuminate these differences, and that the shift of the peak of the observed absorption band from the isolated-atom frequency provides a convenient quantitative measure of these differences, since it is closely related to an extremum in the difference potential. We have therefore tabulated these shifts in Table II for Cs with Ne, Ar, Kr, and Xe. The disagreement between experiment and theory is substantial for all the gases, but is particularly large for Ne and Xe. We have previously[4] compared the positions of the $7s\Sigma$ peaks as observed in emission for Xe, Kr, and Ar with these theoretical potentials from a standpoint that did not require that they be associated with extrema in the difference potentials, with similar results. This did allow a comparison in the case of CsAr, where there is no extremum in the theoretical potential difference—it decreases monotonically in the region of interest.

The disagreement between theory and experiment is even more dramatic in the case of the Rb–noble-gas systems. The large hump in the theoretical $6s\Sigma$ potential shown in Fig. 9 would result in a continuous absorption band extending to 2766 cm^{-1} to the blue of the isolated-atom transition frequency, where we would expect a peak due to the extremum in the difference potential.

TABLE II. Shift of the peak of the Cs–noble-gas absorption band from the forbidden atomic Cs transition in cm^{-1} (experimental), computed from the wavelengths in Table I. The peaks are interpreted as stemming from extrema in the difference potentials. The entries in the theoretical column are the shifts of the extrema in the theoretical difference potentials computed from the adiabatic potential curves of Pascale and Vandeplanque, Ref. 19.

	$7s\Sigma$-$6s\Sigma$		$5d\Sigma$-$6s\Sigma$	
	Expt.	Theor.	Expt.	Theor.
Xe	−1061	−136	1082	3153
Kr	−829	−676	1204	2696
Ar	−741	··· [a]	1478	1759
Ne	−500	217 [b]	1585	3378

[a] No extremum—decreases monotonically.
[b] Two other extrema at 242 and 1060 cm^{-1}.

In other words, we would expect to see a band similar in appearance to the Cs–noble-gas bands shown in Fig. 5. In addition, there might be a second peak with a smaller blue shift due to the second extremum (local minimum) in the difference potential at smaller R. On the contrary, in the case of Rb-Xe the only peak we observe which can be attributed to the $6s\Sigma$ term is *red* shifted by 211 cm^{-1} from the wavelength corresponding to the forbidden $6S$-$5S$ transition, 4966 Å. The middle peak is attributed to the $4d\Sigma$ term, and the red-shifted band to the other terms correlated with the $4D$ state in atomic Rb. For the lighter noble gases the first peak is slightly blue shifted, but in no case do we observe absorption bands with the large blue shifts expected from the PV $6s\Sigma$ potentials (see Fig. 9). For the case of RbXe, a potential qualitatively like that shown by the dotted line in Fig. 9 would be compatible with this analysis of the spectra. We have not studied the temperature dependence of the magnitude of the Rb–noble-gas bands, but we do not see a shift in the wavelength of the peaks with temperature.

We have also observed these bands in emission, both laser excited and in microwave discharge,[21] for both Rb and Cs. The peaks occur at the same wavelengths and the emission spectra are qualitatively consistent with our interpretation of the absorption spectra. There is a simple relation between the emission and absorption spectra at the same temperature,[1] but we have not made a quantitative comparison at this time because the temperature is quite uncertain for the emission case due to an indeterminate amount of heating by the laser beam or the microwaves. The relative excitation of the S and D correlated states is also uncertain in emission.

It is also interesting to note that the shape of the red-shifted absorption bands correlated with the D states in Rb and Cs, which peak close to the forbidden transition wavelength and then fall off gradually with increasing red shift, is quite different from the bands correlated with S states. This indicates that the dependence of the transition moment on R is different for the two cases, and/or that the $d\Pi$ potential curves are more attractive at small R, so that the difference potential decreases monotonically and sharply at small R instead of reaching a minimum and then turning up. A more precise study of the temperature dependence of these bands in absorption or emission might shed some light on this matter. We looked at the temperature dependence primarily in Cs, and our Cs–noble-gas spectra are very uncertain in this region (as we have indicated by using dashed lines in Fig. 5) because of the underlying Cs_2 absorption bands.

SUMMARY AND CONCLUSIONS

Transitions between the ground $^2S_{1/2}$ and excited S and D states in alkali atoms, which are forbidden in isolated atoms, become allowed molecular transitions when the alkali atom is very near a noble-gas atom. We have measured the reduced absorption coefficient of molecular bands associated with these transitions in Cs and Rb in the visible and near infrared and find peak magnitudes on the order of 4×10^{-38} cm^5. The most prominent bands in the spectra are associated with Σ-Σ transitions in the alkali–noble-gas molecules and terminate in peaks which we associate with extrema in the difference potentials. The wavelengths at which these bands and peaks occur, together with an experimental upper bound on the temperature dependence of the absorption coefficient and ground-state potential curves determined by others, are used to deduce some of the properties of the CsXe excited-state Σ potential curves. A comparison is made with the adiabatic potential curves recently calculated by Pascale and Vandeplanque. Their potentials exhibit striking perturbations and avoided crossings in the corresponding excited $s\Sigma$ and $d\Sigma$ potential curves. This structure in the theoretical curves is a result of the strongly repulsive nature of the excited Σ terms, which are uniquely sensitive at relatively large R to a certain repulsive pseudopotential term in their effective Hamiltonian. The comparison with the absorption spectra indicates that the theoretical excited Σ states exhibit too much repulsion.

ACKNOWLEDGMENT

We thank Dr. Alan Gallagher for helpful conversations.

---

*Work supported by the Air Force Office of Scientific Research under Grant No. AFOSR-74-2685, with supplementary support by the Joint Services Electronics Program (U. S. Army, U. S. Navy, and U. S. Air Force) under Contract No. DAAB07-74-C-0341.

[1]R. E. M. Hedges, D. L. Drummond, and A. Gallagher, Phys. Rev. A 6, 1519 (1972).

[2]A. Tam, G. Moe, W. Park, and W. Happer, Phys. Rev. Lett. 35, 85 (1975).

[3]W. Happer, G. Moe, and A. C. Tam, Phys. Lett. 54A, 405 (1975).

[4]A. C. Tam, G. Moe, B. R. Bulos, and W. Happer, Opt. Commun. 16, 376 (1976).

[5]M. Lapp and L. P. Harris, J. Quant. Spectrosc. Radiat. Transfer 6, 169 (1966).

[6]A. E. Wechsler, Dept. of Defense (U.S.) Document No. AD-631469, 1966 (unpublished).

[7]R. W. Ditchburn and J. C. Gilmour, Rev. Mod. Phys. 13, 310 (1941); see also the review by W. H. Wilson, in *Mellor's Comprehensive Treatise on Inorganic and Theoretical Chemistry, Volume II, Supplement III, The Alkali Metals Part 2* (Longmans, London, 1963), p. 2294.

[8]J. Granier and R. Granier, J. Quant. Spectrosc. Radiat. Transfer 13, 473 (1973); J. G. Eden, J. T. Verdeyen, and B. E. Charrington, Bull. Am. Phys. Soc. 21, 168 (1976).

[9]This ratio is determined experimentally from our absorption curves for Cs with no noble gas present and is consistent with the $[Cs_2]/[Cs]$ curve in Ref. 5.

[10]M. Lapp, Phys. Lett. 23, 553 (1966).

[11]J. A. Gwinn, P. M. Thomas, and J. F. Kielkopf, J. Chem. Phys. 48, 568 (1968).

[12]F. Besombes, J. Granier, and R. Granier, Opt. Commun. 1, 161 (1969).

[13]J. Granier, R. Granier, and F. Schuller, J. Quant. Spectrosc. Radiat. Transfer 15, 619 (1975).

[14]D. L. Drummond and A. Gallagher, J. Chem. Phys. 60, 3426 (1974).

[15]G. York, R. Scheps, and A. Gallagher, J. Chem. Phys. 63, 1052 (1975).

[16]J. Szudy and W. E. Baylis, J. Quant. Spectrosc. Radiat. Transfer 15, 641 (1975).

[17]K. M. Sando and J. C. Wormhoudt, Phys. Rev. A 7, 1889 (1973); K. M. Sando, *ibid.* 9, 1103 (1974).

[18]C. G. Carrington and A. Gallagher, Phys. Rev. A 10, 1464 (1974).

[19]J. Pascale and J. Vandeplanque, J. Chem. Phys. 60, 2278 (1974); J. Pascale and J. Vandeplanque, Molecular Terms of the Alkali–Rare-Gas Atom Pairs, CEA Reports, Saclay, France, 1974 (unpublished).

[20]W. E. Baylis, J. Chem. Phys. 51, 2665 (1969); W. E. Baylis, Joint Institute for Laboratory Astrophysics Report No. 100, Univ. of Colorado, 1969 (unpublished).

[21]Andrew C. Tam and George W. Moe, Phys. Rev. A (to be published).